

1 **Using Frequency Response Function Testing to examine a Railway Trackbed**

2 R De Bold, D Connolly, S Patience & Professor MC Forde

3 University of Edinburgh

4 School of Engineering

5 AGB Building

6 The Kings Buildings

7 Edinburgh EH9 3JL, UK

8

9 r.de-bold@ed.ac.uk ; m.forde@ed.ac.uk

10 **WORD COUNT**

11 Actual text: 4,500 words.

12 Figures and tables: 12 (at 250 “words” each = 3,000 “words”).

13 Effective paper length: 7,500 “words”.

14 **KEYWORDS**

15 Railway Maintenance, ballast, spent, fouling, analysis, testing, impulse, response

1 **ABSTRACT**

2 The increase in both freight and passenger rail travel has driven the demand for more
3 efficient and rapid investigation of railway trackbed ballast.

4 One of the current approaches to evaluating the stiffness of railway ballast is to use a
5 Falling Weight Deflectometer. Whilst this is very effective, it requires the rails to be
6 unclipped from the ties – thus, it is very intrusive and expensive.

7 This paper explores the option of using a frequency response function (FRF)
8 generated by using a 12lb instrumented hammer to excite the railway trackbed.

9 Finally, the FRF is correlated with the ballast fouling.

1 INTRODUCTION

2 Highway congestion and the sustainability agenda are driving the increased demand for more
3 rail travel. This in turn has driven the demand for more efficient and rapid investigation of
4 railway trackbed ballast. The objectives of this paper are: -

- 5 1. To develop a procedure for simply and cost effectively measuring ballast fouling
6 using a frequency response function (FRF); and,
- 7 2. To relate this stiffness measurement to ballast fouling.

8 CURRENT STATE OF PRACTICE

9 The permanent way structure is traditionally composed of a superstructure and substructure.

10 The ballast supports stresses imposed upon the rails and maintains their correct
11 position. Furthermore, the ballast structure, featuring large voids, provides for necessary
12 drainage.

13 However, ballast deteriorates over time through a process of degradation, where the
14 particles mechanically interact, or weather, and change shape; or, through fouling, where fine
15 particles accumulate in the void structure. Subsoil intrusion is a major source of fouling, as
16 are wind and waterborne sources that vary with localised environmental conditions. Such
17 deteriorated ballast is defined as “spent” and fails to provide the drainage and mechanical
18 functions required.

19 Identification of spent ballast is often undertaken visually, but this can be unreliable.
20 One of the most reliable ways to determine ballast condition is to take a sample and to
21 undertake a particle size distribution analysis as per ASTM or BS (1). This is time
22 consuming, laborious, requires track possession, and, therefore, is seldom used. If one waits
23 for ballast symptoms to become obvious, then the maintenance regime to deal with
24 deterioration is a reactive one, and, consequently, cost-inefficient. Ground penetrating radar
25 (GPR) (2) is a non-destructive evaluation (NDE) technique to evaluate ballast condition and
26 involves measuring signal reflections of radar pulses transmitted into the ground. It is still
27 being researched and is now partially deployed commercially.

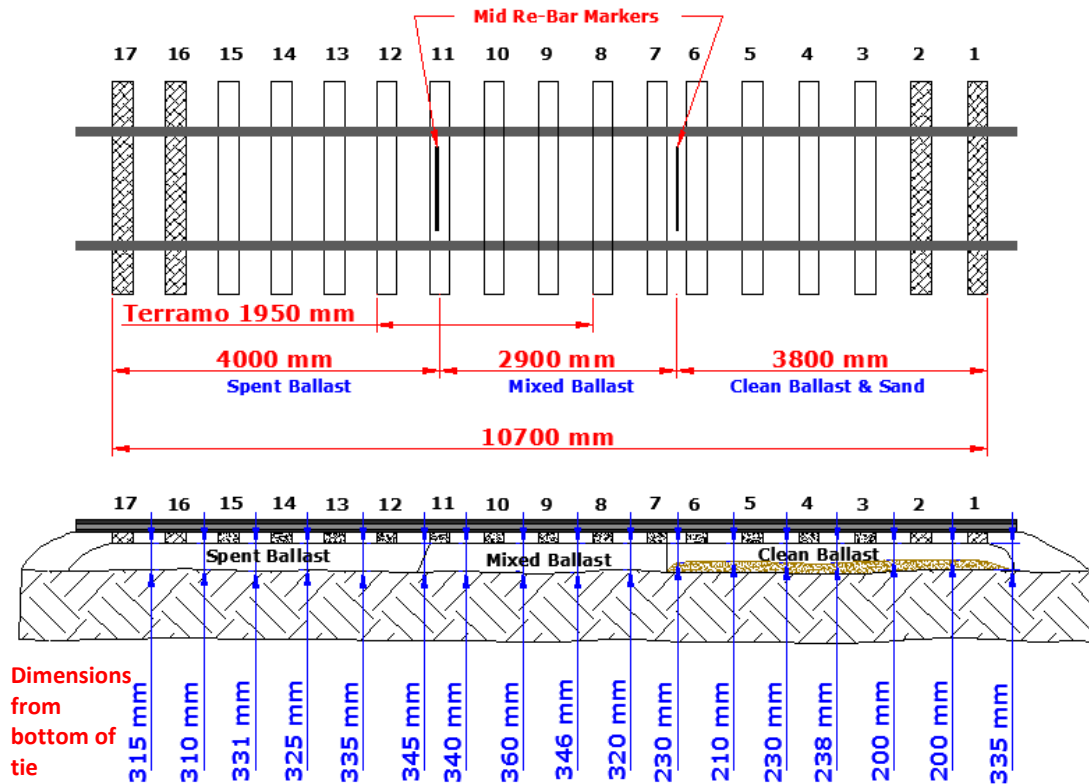
28 An NDE technique to examine ballast stiffness is the Falling Weight Deflectometer
29 (FWD). An FWD involves dropping a known mass onto the track and measuring the track’s
30 response. The apparatus is large, requires disconnection of clips from sleepers or ties over
31 sections of track and, thus, track possession. In an FWD, there is a built-in geophone, which
32 only permits vibration measurement of the same track component on which excitation takes
33 place. Therefore, the FWD apparatus is not used to impact the tie, or other track components,
34 and measure the ballast vibration.

35 There is thus an opportunity to provide a track ballast stiffness evaluation tool that is
36 less intrusive, low cost, can quickly appraise areas of track in a short period of time, and give
37 a fingerprinting result from which time-to-maintenance can be calculated and planned. An
38 impulse response technique will be discussed in this paper.

39 TESTING

40 Impulse response tests were conducted on the University of Edinburgh railway track test bed
41 (Figure 1).

42 A section of full scale trackbed was constructed at the University of Edinburgh as part
43 of an earlier project (3). The track is full-scale, 10m long, and built to British Rail Standard
44 BR1203 – except that along its length, increasingly spent ballast was used.



1 **Figure 1 Full-scale trackbed facility (3)**

2 An instrumented 12lb impact-impulse hammer with built-in load cell that converted
 3 the impact force into an electrical signal was used to impact various parts of the track and the
 4 vibration response was recorded using a nearby transducer. The 12lb hammer was chosen
 5 over smaller models because it imparts the largest force and has the lowest frequency content
 6 (4). Two different hammer tips were used, one made from rubber and one made from vinyl.

7 A velocity transducer (geophone) and a displacement transducer were used to record
 8 the hammer impact responses. Later analysis found that the displacement transducer data
 9 was not suitable as the low frequency performance was less linear. The geophone used was a
 10 low frequency model and captured the data of interest, ie, less than 100Hz, whereas the
 11 displacement transducer did not.

12 A National Instruments dynamic signal conditioning unit with USB connectivity was
 13 used to supply power and condition the signals from the hammer and geophone. National
 14 Instruments software was used to record the data on a laptop PC. A programme was
 15 constructed with the software to manage the devices and collect, analyse, display, and record
 16 the data.

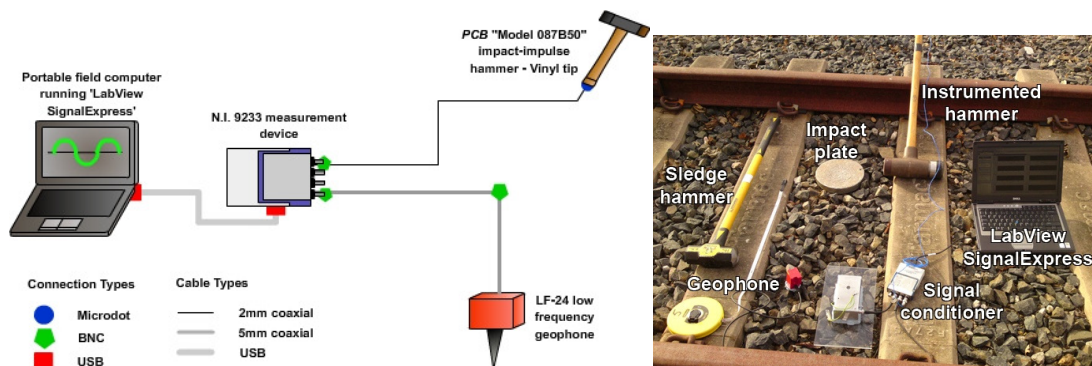
17 The general testing procedure for each crib was to impart a force onto the structure
 18 using both the vinyl and rubber hammer tip with the geophone located at a distance of
 19 500mm (this distance was found to produce the clearest and most consistent results). The test
 20 was repeated three times at cribs 1, 2, 3, 4, 6, 8, 10, 12, 14, and 16.

21 The three main structural components were tested using the following setup
 22 configurations:

- 1 **Setup 1** Ballast impacted with hammer and response from ballast measured
2 – “Hit Ballast, Measure Ballast”.
- 3 **Setup 2** Ballast impacted with hammer and response from tie measured
4 – “Hit Ballast, Measure Tie”.
- 5 **Setup 3** Ballast impacted with hammer and response from rail measured
6 – “Hit Ballast, Measure Rail”.
- 7 **Setup 4** Rail impacted with hammer and response from ballast measured
8 – “Hit Rail, Measure Ballast”.
- 9 **Setup 5** Tie impacted with hammer and response from ballast measured
10 – “Hit Tie, Measure Ballast”.

11 When the impulse hammer was impacted on the ballast, a metal strike plate was used
12 for the hammer on the ballast. This would be bedded into the ballast with a sledgehammer
13 prior to testing.

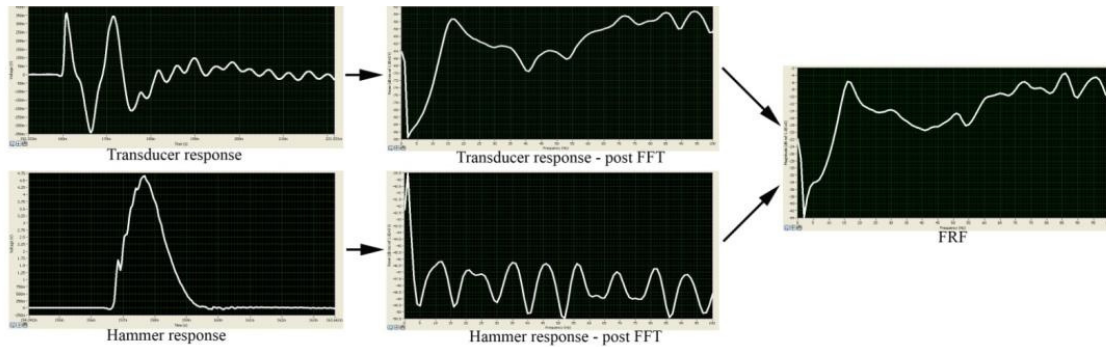
14 When the response from the ballast was measured, the geophone would be affixed to
15 a 15cm spike with a square flat head that would be driven into the ballast with a
16 sledgehammer prior to testing. A 2mm thick strip of plasticine was used as an effective
17 coupling material (5). The experimental setup is shown in Figure 2.



18 **Figure 2 Experimental setup schematic and photograph**

19 **Signal Analysis**

20 The analysis software converted the hammer and transducer responses from the time domain
21 into the frequency domain using a Fast Fourier Transform (FFT). The transducer FFT
22 response was divided by the hammer’s FFT response in order to produce the Frequency
23 Response Function (FRF) (Figure 3).



1 **Figure 3 FRF calculation process**

2 The FRF discards the effects of magnitude and type of loading (6) meaning that the
 3 low frequency content can be related to track stiffness.

4 **TRACKBED ANALYSIS**

5 Since construction in 1999, the test track has undergone physical changes that can be
 6 attributed to weather conditions and experimentation. An analysis of the ballast condition
 7 was undertaken by means of a PSD analysis in order to determine the ballast deterioration.

8 From the PSD results the fouling index for each crib was calculated. There are two
 9 methods for calculating ballast deterioration - Selig, et al, 1994 (7) and Ionescu, 2004 (8).
 10 The latter adheres to Australian standards that are similar to the material parameters used in
 11 British trackbed construction. Since the trackbed was constructed to BR1203 specifications,
 12 the Ionescu method was used: -

$$F_I = P_{0.075} + P_{14} \quad \text{Where:} \quad \begin{array}{l} F_I = \text{Fouling index} \\ P_{0.075} = \% \text{ passing } 0.075\text{mm sieve} \\ P_{14} = \% \text{ passing the } 14\text{mm sieve} \end{array}$$

1 The categories of fouling developed by Selig & Waters were used in conjunction with
 2 the derived fouling index formula to determine the condition of the test track. Applying
 3 Ionescu's formula to the collected data returns the following results:

4
 5 **Table 1 Ballast fouling index**

Crib No.	F_1	Category
1	1.60%	Moderately Clean
2	1.74%	Moderately Clean
3	1.41%	Moderately Clean
4	1.06%	Moderately Clean
5	2.40%	Moderately Clean
6	1.36%	Moderately Clean
7	4.41%	Moderately Clean
8	10.74%	Moderately Fouled
9	14.89%	Moderately Fouled
10	11.50%	Moderately Fouled
11	1.93%	Moderately Clean
12	22.23%	Fouled
13	24.94%	Fouled
14	15.90%	Moderately Fouled
15	17.06%	Moderately Fouled
16	30.73%	Fouled

6 A limitation of such a fouling index is that it is only a function of spentness of the
 7 ballast. This is because fouling index is solely a description of the fines content of a particular
 8 ballast sample but spentness is a description of a collection of various other variables such as
 9 fines content, drainage efficiency, and surface texture (9).

10 **CURRENT METHODS OF STIFFNESS MEASUREMENT**

11 **The Definition of Stiffness**

12 The two main characteristics of spent ballast are a reduction in strength and stiffness. If track
 13 stiffness can be quantified, then, as it is related to ballast condition, the spentness of the
 14 ballast can be established.

15 Stiffness (K) is defined as “the ratio of a steady force (P) acting on a deformable
 16 elastic medium to the resulting displacement” (10). This means that if the track is stiff, then
 17 when a train passes, the track deformation will be low; and if the track is non-stiff, then when
 18 a train passes, the track deformation will be high.

19 **Impulse Response**

20 A well-documented area of research to determine the stiffness of concrete structures is
 21 impulse response testing where an instrumented hammer is used to excite a structure and the
 22 response of the structure is measured with a transducer. There are many different hammer
 23 sizes and tip materials available.

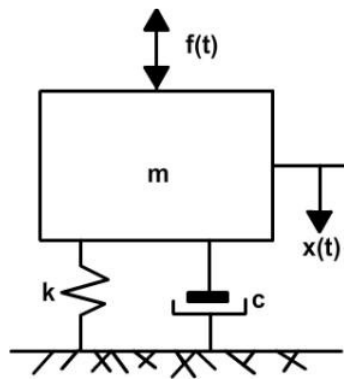
1 Measurements are recorded in the time domain and converted into the frequency
 2 domain using a Fast Fourier Transform (FFT) algorithm. When the response is measured
 3 using a geophone, the velocity values are divided by the hammer response to obtain an FRF
 4 in terms of mechanical admittance (or, “mobility”).

5 In general, if the tip is constructed from a hard material then the hammer will have a
 6 shorter contact time and will impart higher frequencies. If it is soft, then it will impart lower
 7 frequencies. For the purposes of impulse response, a low enough frequency must be used so
 8 that the structure responds to the impact in a bending mode rather than a reflective mode (11).

9 **The Mass-Spring Model**

10 The mass-spring model is used to describe the vertical support condition of the track. It
 11 assumes that the rail and ties are continuously supported beams supported by mass-less
 12 springs. Therefore, it can be used to describe how the track structure responds to excitation.

13 The ballast can be thought of as a Single Degree of Freedom (SDoF) system (Figure
 14 4), meaning that when it is vertically excited, horizontal and lateral movement can be taken
 15 as zero. Therefore, the ballast is considered to be only moving in one direction, vertically.



Where: c = damping co-efficient
 m = mass of the entire system
 k = stiffness of the spring

16 **Figure 4 Mass-spring model of an SDoF system**

17 The force applied to the mass represents the hammer blow and is defined as $f(t)$, and
 18 the mass’s position is defined solely in the vertical axis by $x(t)$.

19 Therefore, the general equation of motion is: -

$m\ddot{x} + c\dot{x} + kx = -m\ddot{y}$	Where,	x = displacement
Or		\dot{x} = velocity
$m\ddot{x} + c\dot{x} + kx = f(x)$		\ddot{x} = acceleration

20 **The Impulse Response Method**

21 Previous research has analysed the mass-spring system using the excitation force and the
 22 structural response to derive the FRF to determine concrete material properties (12).
 23 Therefore, to calculate ballast stiffness the mass-spring model needs to be further developed
 24 (6).

25 For the case of no damping, the FRF is calculated with the damping force considered
 26 to be zero.

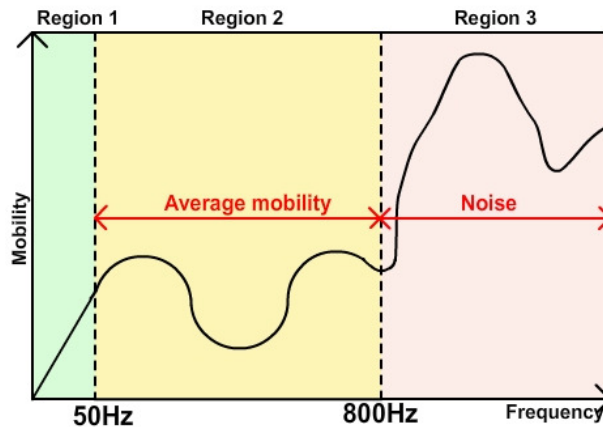
27 If no excitation force is applied, then $f(t) = 0$ and $c\dot{x} = 0$

1 So the equation of motion becomes..... $m\ddot{x} + kx = 0$
 2 Which has the solution..... $x = -e^{-i\omega t}$
 3 Now, consider an excitation of the form $f(t) = fe^{i\omega t}$
 4 Then, using trial solution (x independent of time and
 5 contains information on phase and magnitude) $x(t) = xe^{i\omega t}$
 6 Gives $k - \omega^2 m = 0$
 7 Therefore, the modal model consists of one mode of
 8 vibration with a natural frequency given by $\omega_0 = \left(\frac{k}{m}\right)^{0.5}$
 9 The equation of motion then becomes..... $(k - \omega^2 m)xe^{i\omega t} = fe^{i\omega t}$
 10 Therefore, this can be solved and is the equivalent to the ballast vibration divided by
 11 the input: -

$$\alpha(\omega) = \frac{x}{f} = \frac{1}{k - \omega^2 m} = \frac{\text{Transducer response}}{\text{Hammer response}} \quad \text{Equation 1}$$

12 **The Application of Impulse Response Testing to Ballast**

13 A typical FRF of a concrete structure can be broken down into three regions (13) (Figure 5): -



14 **Figure 5 Characteristics of an FRF**

- 15 **Region 1** 0 to 50 or 100Hz – defines the static compliance and is directly related to
- 16 stiffness.
- 17 **Region 2** 100 to 800Hz – the average mobility value inside this range is related to
- 18 stiffness.
- 19 **Region 3** Above 800Hz – data in this region not related to stiffness.

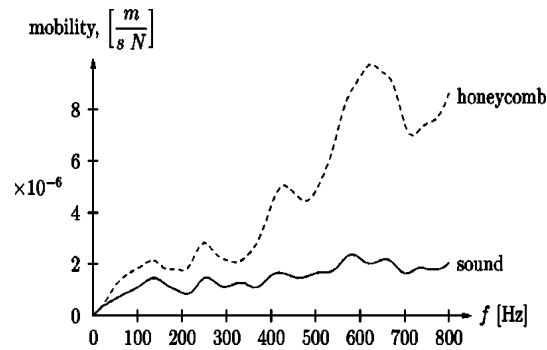
1 If the FRF of the ballast is found, then this equation can be used to find the dynamic stiffness
 2 from the initial gradient (13).

3 Other research concluded that dynamic stiffness is calculated using (14):

$$E' = \frac{2\pi}{M} \quad \text{Where,} \quad \begin{array}{l} E' = \text{dynamic stiffness} \\ M = \text{gradient of initial low} \\ \text{frequency part of FRF} \end{array} \quad \text{Equation 2}$$

4 It is further explained that when a structure is excited at low frequencies, the inertia
 5 effects are negligible causing the structure to behave like a spring, and that the initial slope up
 6 to 100Hz defines the structures static compliance and that the slope's inverse is equal to the
 7 dynamic stiffness (16).

8 Later research into concrete tunnel linings found that the gradient to 50Hz (13) is the
 9 range over which stiffness can be calculated, and further states that there is a difference in
 10 FRF response between "honeycombed" concrete and "sound" concrete (Figure 6). Ballast
 11 contains many voids and, therefore, this method could be applicable to ballast if one
 12 considers clean ballast analogous to honeycombed concrete and spent ballast analogous to
 13 sound concrete.



14 **Figure 6 Typical FRF of honeycombed and sound concrete (13)**

15 Continuation of the research into concrete tunnel linings looked at other structural
 16 properties that can be determined from an FRF plot (1). This found that the mean mobility
 17 over the 100-800Hz range can also be used as an indicator of stiffness.

18 Historical research on vibration testing of piles used the gradient of the initial
 19 mobility line before the first peak on a mobility plot to calculate stiffness (14). Through
 20 visual inspection, it was found that this peak occurred at 18Hz on tests at the Edinburgh track
 21 using a vinyl tipped hammer.

22 Similarly, the previous method that used the mean mobility over 100-800Hz range,
 23 used the 100Hz value as this was where the first peak in the mobility graph occurred. If this
 24 method is scaled, given that the first peak in the Edinburgh track experiments occurs at 16Hz,
 25 then, if the relationship is considered to be linear, then a range of 18-128Hz may be more
 26 appropriate for the Edinburgh track using this method.

27 Chan, 1987 (15), showed that a 10dB drop in the hammer response is used to
 28 determine the upper limit in the useful range of frequencies to determine stiffness. The most
 29 important criteria in deciding this useful range is the minimal loss of power. This could give
 30 an alternative method to calculate the upper limit with each test visually inspected and a
 31 useful frequency range determined.

1 Therefore, from the FRF of ballast, it may be possible to determine its stiffness using
2 these methods. However, these assessments are based on research into concrete structures
3 being excited with a 1kg hammer with an aluminium tip.

4 Testing on the Edinburgh track was undertaken with a 12lb hammer with vinyl and
5 rubber tips. Therefore, the nature of the excitation forces imparted on the ballast will be
6 considerably different.

7 **Summary of Theories**

8 To investigate the application of impulse response on railway ballast, an FRF was calculated
9 for most cribs of the Edinburgh track and the noted theories for relating stiffness to the FRFs
10 were investigated: -

11 **Theory 1** Stiffness is related to gradient of initial line between 0-50Hz on FRF plot.

12 **Theory 2** Stiffness is related to gradient of initial line between 0-100Hz on FRF plot.

13 **Theory 3** Stiffness is related to average mobility between 100-800Hz on FRF plot.

14 **Theory 4** Stiffness is related to gradient of initial line between 0-18Hz on FRF plot.

15 **Theory 5** Stiffness is related to average mobility between 18-128Hz on FRF plot.

16 **Theory 6** Stiffness is related to average mobility on FRF plot defined by: -

17 Lower limit = 18Hz

18 Upper limit = Established empirically from hammer response spectrum.

19 **COPONENT DATA ANALYSIS**

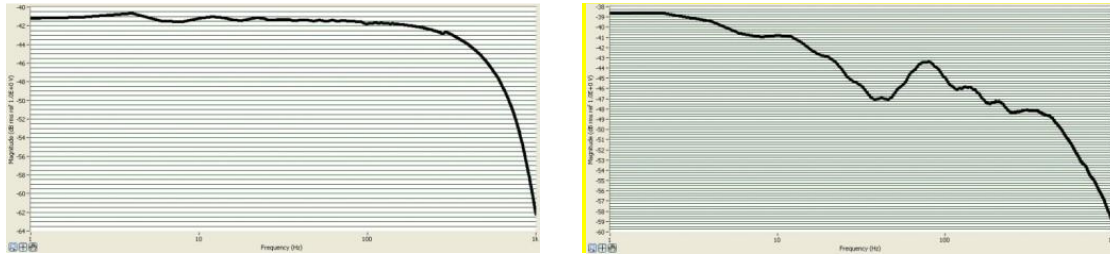
20 **Hammer tip analysis**

21 A method to determine the maximum frequency to which an instrumented hammer tip is
22 accurate, is to determine in the frequency domain a 10dB drop in the hammer response (15).
23 Data collected at higher frequencies contained too much spurious and unreliable.

24 Different power spectra (FFT of the hammer response) are produced by different
25 hammer tip materials. Softer tips, eg, rubber, are only accurate to lower frequencies.
26 Therefore, FRFs can only be accurate to the instrumented hammers useful frequency range.

27 In the experiments, the instrumented hammer was used to impart force onto three
28 different components (made of four different materials): rail (steel), tie (concrete or wood),
29 and ballast (crushed stone). The power spectra for the ballast and ties were found to be
30 distinctly different. This was found to be the case for both vinyl and rubber tips; although,
31 for consistency this discussion will focus on the vinyl tip.

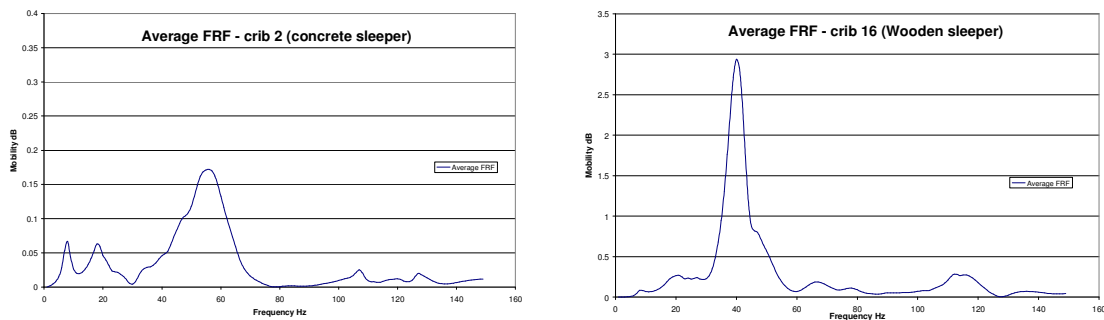
32 However, the material impacted also has an effect on the quality of the response.
33 Figure 7 shows that the log-log scale power spectrum responses for a concrete tie and ballast.
34 The concrete tie response is a horizontal straight line until about 100Hz and then it decreases
35 rapidly; this is in contrast to the response for ballast, which decreases more irregularly.



1 **Figure 7 Power spectra for concrete tie (left) and ballast (right) – vinyl tip**

2 The wooden tie exhibited a different useful frequency range in comparison to the
 3 other materials. For a concrete tie, the 10dB drop occurred around 600Hz, but for the
 4 wooden tie it occurred around 300Hz. This is because “variations in the [useful frequency
 5 range] values are expected due to changes in hardness of material” (15). This means that the
 6 useful frequency range is a function of both the hammer tip and the impact material.
 7 Therefore, at low frequencies, the contact between the vinyl tip and concrete has a higher
 8 degree of accuracy.

9 The magnitude of the force that the tie absorbs from the hammer also has an effect on
 10 the resulting FRF. The power spectrum for the wooden tie response is generally higher than
 11 the concrete tie, meaning that whenever the FRF is calculated, the average mobility value is
 12 larger for the wooden tie (Figure 8). This large discrepancy meant that it was impractical to
 13 analyse the FRFs for the concrete and wooden ties together.



14 **Figure 8 FRF for concrete tie (left) and wooden tie (right)**

15 MOBILITY ANALYSIS

16 Hammer Tip Selection

17 The ballast was excited using both the hammer’s vinyl and rubber tips. Both tips were
 18 analysed to determine how they compared with the findings from the soil classification tests.
 19 The general trend was that the vinyl tip results had a stronger correlation with the fouling
 20 index values. Therefore, theory comparisons are analysed with the vinyl tip results.

21 Testing

22 Each theory was tested to determine a stiffness value for each crib using each test setup.
 23 Then to determine the closeness of results, the stiffness values were compared to the results
 24 from the soil classification tests using the Pearson Product Moment correlation co-efficient.

25 The Pearson correlation co-efficient describes the quality of the correlation between
 26 the impulse response test results and fouling index. The strength of the correlation is

1 represented by a number between -1 and 1 where ‘1’ indicates a strong positive linear
 2 relationship, “0” indicates zero linear relationship and -1 indicates a strong negative linear
 3 relationship: -

$$\rho_{x,y} = \frac{n \sum x_i \sum y_i - \sum x_i \sum y_i}{\sqrt{n \sum x_i^2 - (\sum x_i)^2} \sqrt{n \sum y_i^2 - (\sum y_i)^2}} \quad \text{Equation 3}$$

4 The impulse response data for Cribs 1 and 16 was discarded and not used in
 5 correlation calculations in all cases except for test Setup 1. This was because of the presence
 6 of either a rail discontinuation or a wooden tie.

7 Summary of Results

8 A summary of the results is noted in Table 2: -

9 **Table 2 Theories 1-5 Vs fouling index**

Test Setup	Impact Comp	Measured Comp	Theory 1	Theory 2	Theory 3	Theory 4	Theory 5
			50Hz Gradient Correl	100Hz Gradient Correl	100-800Hz Ave Val Correl	16Hz Gradient Correl	18-128Hz Ave Val Correl
1	Ballast	Ballast	-0.57	-0.53	0.18	-0.76	-0.54
2	Ballast	Sleeper	-0.46	0.05	0.16	-0.49	-0.02
3	Ballast	Rail	-0.54	-0.43	0.42	0.01	-0.37
4	Rail	Ballast	-0.57	-0.25	-0.41	-0.51	-0.30
5	Sleeper	Ballast	-0.88	-0.50	-0.49	-0.41	-0.61

10

Table 3 Best correlations

Test Setup	Impact Comp	Measured Comp	Theory 6		Best Range	
			Empirical Range		Range (Hz)	Ave Val Correl
			Range (Hz)	Ave Val Correl		
1	Ballast	Ballast	18-70	-0.61	18-50	-0.81
2	Ballast	Sleeper	18-70	-0.44	18-48	-0.65
3	Ballast	Rail	18-95	-0.17	18-44	0.48
4	Rail	Ballast	18-60	-0.51	18-58	-0.52
5	Sleeper	Ballast	18-60	-0.94	18-60	-0.94

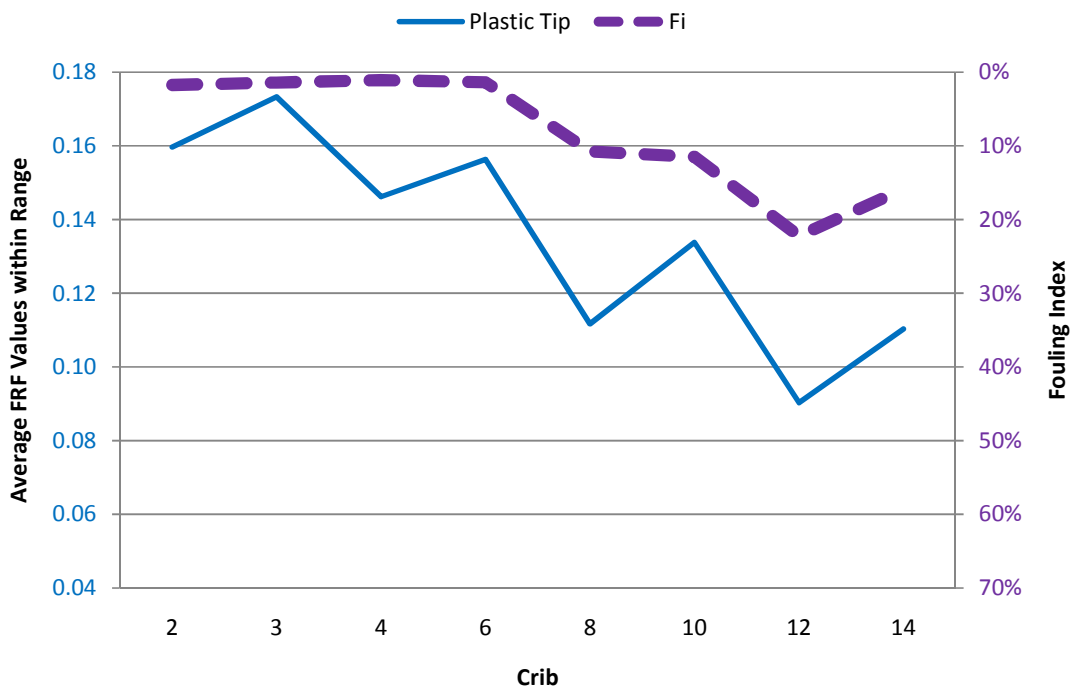
11 The correlation between Theories 1 to 5 and the fouling index for each crib is shown
 12 in Table 2. The majority of the correlations are negative indicating a negative relationship
 13 between the two variables, thus giving some credence to the analogous comparison of clean
 14 ballast to honeycombed concrete and spent ballast to sound concrete. The correlation
 15 between the initial 50Hz gradient and fouling index is low for each testing condition except
 16 when the tie was excited and the ballast vibration measured. In this case, the correlation
 17 coefficient is -0.88.

1 The correlations with Theory 2, 3, 4, and 5 and the fouling index is significantly
 2 smaller in magnitude than -0.88 for all other testing combinations, thus serving as poor
 3 indicators of ballast condition.

4 Significantly improved correlations are found by applying Theory 6 of calculating the
 5 average mobility values between the first peak (18Hz) and a maximum frequency determined
 6 by a 10dB drop in the hammer FFT (Table 3).

7 The results were also analysed to find the best correlations possible by varying the
 8 frequency range used (without any rationale as to why that frequency range was used (Table
 9 3)).

10 For Setup 5 (“Hit Tie, Measure Ballast”), this has a correlation of -0.94, which is
 11 considered to be significant (Figure 9).



12 **Figure 9 Hit tie, measure ballast results**

13 **Linearity**

14 According to Ewins (1984) (6), some aspects of impulse response testing rely on the test
 15 structure having a high degree of “linearity”. Linearity is related to the complexity of the test
 16 structure and without it, some of the relationships associated with modal testing are invalid.

17 There are three signs of non-linear behaviour: -

- 18 • Natural frequencies vary with strength and position of excitement;
- 19 • Distorted FRFs; and,
- 20 • Unrepeatable or unstable data.

21 The main way to check for non-linearity is to test the structure in question several times
 22 using different magnitudes of excitation. If the resulting FRFs exhibit large discrepancies,
 23 especially in areas of resonance then it is possible that the structure’s behaviour is non-linear.

1 From the individual test data (see appendices), it can be seen that the greatest
 2 repeatability of results are for test Setup 5 – “Hit Tie, Measure Ballast”. This would lend
 3 credence to the notion that it is more “linear” and, therefore, able to be impulse response
 4 tested.

5 It is considered that when the ballast is excited directly (Setup 1, 2, and 3), it acts non-
 6 linearly and this non-linearity is recorded by the geophone. This is caused by the complex
 7 and random arrangement of crushed stone that make up the ballast structure. The poor
 8 performance of Setup 4 – “Hit Rail, Measure Ballast” could be considered due to the
 9 complexity of the arrangement of the impact force travelling through the rail, then tie, and
 10 then into the ballast.

11 **The Receptance Effect**

12 It can be proven mathematically that only receptance (an FRF from a displacement transducer
 13 rather than a velocity transducer) can provide a method of calculating stiffness (6). It is
 14 proposed that the reason mobility is a strong indicator of stiffness is because the mean
 15 mobility over a given range is directly related to receptance. Therefore, calculating the mean
 16 mobility value over a given range is very similar to integrating mobility over the same range.

17 This theory was tested and the mean mobility was plotted against integrated mobility
 18 over the 18-60Hz range. The values obtained were very similar but the integrated values
 19 were all almost exactly 36 times larger than the mean mobility. Thus, the integrated mobility
 20 values correlated just as well with the fouling index as the mean mobility values.

21 **Mapping average mobility to fouling index**

22 Test Setup 5 has a -0.94 correlation with the fouling index values meaning that it could
 23 provide a high-quality estimate of ballast condition. This strong correlation coefficient
 24 suggests that it might be possible to establish a basic relationship mapping impulse response
 25 test results to fouling index; thus: -

- 26 • According to Ottosen (2004) (17), Average mobility \propto Stiffness
- 27 • And if, Stiffness \propto Spentness
- 28 • And, Spentness \propto Fouling index
- 29 • Then Average mobility \propto Fouling index

30 **CONCLUSIONS**

31 An experimental study was conducted to establish correlations between ballast stiffness when
 32 excited by a modally tuned instrumented hammer, using the Frequency Response Function
 33 Method (FRF).

34 The strongest mobility correlation was exhibited when the tie was impacted and the
 35 ballast vibration measured. This high correlation was attributed to the hardness and high
 36 linearity of the concrete ties. No other track component has the same hardness or a high
 37 enough degree of linearity to be capable of reliably predicting ballast conditions.

38 This estimation of ballast stiffness was then successfully correlated with a ballast
 39 fouling index – achieving a correlation coefficient of -0.94.

40 **ACKNOWLEDGMENTS**

41 The authors acknowledge the financial support of EPSRC and the University of Edinburgh;
 42 and Germann Instruments for the loan of instrumentation.

1

2 REFERENCES

- 3 1. BS 1377-2:1990. *Methods for test for soils for civil engineering purposes*, British
4 Standards Institution.
- 5 2. Clark, M, Gordon, MO & Forde, MC (2004) Issues over high-speed non-invasive
6 monitoring of railway trackbed, *NDT&E International*, Elsevier Science, Vol 37, No.
7 2, 131-139, ISSN: 0963-8695
- 8 3. Gallagher, GP (1999) *Investigation of Railway Trackbed Deterioration using Ground*
9 *Penetrating Rada*., MSc Thesis, University of Edinburgh, p. 126
- 10 4. Rausche, F, Likins, G & Shen, RK (1992) Pile Integrity Testing and Analysis, *Proc*
11 *4th Int Conf on the Application of Stress-Wave Theory to Piles*, The Hague
- 12 5. Colombo, S, Giannopoulos, A, Forde, MC, R. Hasson, R, Mulholland, J (2005)
13 Frequency response of different couplant materials for mounting transducers, *NDT &*
14 *E International*, Vol 38, No. 3, April, 187-193, ISSN: 0963-8695
- 15 6. Ewins, DJ (1987) *Modal testing: Theory and practice*. Research Studies Press, 1984
- 16 7. Selig, ET & Waters, JM (1994) *Track Geotechnology and Substructure Management*,
17 Thomas Telford, pp. 2.1-14.1.
- 18 8. Ionescu, D (2004). Ballast degradation and measurement of ballast fouling. *Proc of*
19 *7th Int Conf: Railway Engineering-2004*, London, Engineering Technics Press.
- 20 9. Parker, SP (1997) *Dictionary of Engineering*. 5th Edition, McGraw-Hill, 1997. ISBN
21 0-07-052435-1.
- 22 10. Rasmussen, S & De Man, A (2000) Two new techniques for easurement of vertical
23 track stiffness of railway track, *Proc 3rd Int Conf Railway Engineering-2000*,
24 London, Engineering Technics Press, Edinburgh, ISBN 0-947644-43-1
- 25 11. ACI International (2009) Stress-wave methods for structures, *ACI 228.2R Revision*.
26 *NDT of concrete*, Private Communication
- 27 12. McCavitt, N, Yates, MR & Forde, MC (1992) Dynamic Stiffness Analysis of
28 Concrete Paving Slabs, *ASCE Journal of Transport Engineering*, Vol. 118, No 4, pp.
29 540-556.
- 30 13. Davis, AG, Lim, MK & Petersen, CG (2004) Rapid and economical evaluation of
31 concrete tunnel linings with impulse response and impulse radar non-destructive
32 methods, *NDT&E International*, Vol 38, No. 3, 181-186.
- 33 14. Davis, AG & Dunn, CS (1974) From Theory to Field Experience with the Non-
34 Destructive Vibration Testing of Piles, *Proc of the Institution of Civil Engineers*. Vol.
35 57, No 2, 571-593.
- 36 15. Chan, HFC (1987) *Non-Destructive Testing of Concrete Piles Using the Sonic Echo*
37 *and Transient Shock Methods*, PhD thesis, University of Edinburgh
- 38 16. Davis, A G, Olson, CA & Michols, KA (2001) Evaluation of historic reinforced
39 concrete bridges, *ASCE News*, Vol. 26, No 11, 1-13
- 40 17. Ottosen, N, Ristinmaa, M & Davis, AG (2004) Theoretical interpretation of impulse
41 response tests of embedded concrete structures., 2004, *ASCE Journal of Engineering*
42 *Mechanics*, Vol. 130, No. 9, 1062-71